Computing and Artificial Intelligence 2026, 4(2), 4398.
doi: https://doi.org/10.59400/cai4398

Article

YOLOv26-based automated crater detection and geometric measurement using Chandrayaan-2 Orbiter High Resolution Camera (OHRC) imagery

Meenakshi Sarkar*, **Prit Gajjar**

Space Application Centre, Indian Space Research Organization, Ahmedabad 380015, India

*** Corresponding author:** Meenakshi Sarkar, meenakshi@sac.isro.gov.in

CITATION

Sarkar M, Gajjar P. YOLOv26-based automated crater detection and geometric measurement using Chandrayaan-2 Orbiter High Resolution Camera (OHRC) imagery. Computing and Artificial Intelligence. 2026; 4(2): 4398. https://doi.org/10.59400/cai4398

ARTICLE INFO

Received: 30 January 2026
Revised: 5 April 2026
Accepted: 10 April 2026
Available online: 11 May 2026

Abstract: Accurate detection and measurement of lunar craters are crucial for a better understanding of the geological history and evolution of the Moon's surface. Manually detecting and measuring craters using high-resolution images is not only tedious but may also involve a certain amount of subjectivity. What makes this proposal innovative is the combination of the You Only Look Once (YOLO) algorithm with the Segment Anything Model for accurate segmentation of craters' pixels and measurement of their geometrical properties. In this framework, the locations of the craters are automatically detected using the YOLOv26 algorithm, followed by accurate determination of the crater regions using the Segment Anything Model (SAM). Finally, the accurate determination of the diameter, radius, and surface area of the craters is carried out using the pixel measurement and scale factor conversion technique. This approach will be trained and tested using a dataset comprised of about 12,000 images obtained by dividing the Orbiter High Resolution Camera (OHRC) lunar imagery into image patches of 640 × 640 dimensions and divided in the ratio of training set: validation set: test set as 70:20:10. This model gave a precision value of 91.5%, a recall of 88.6%, mAP@50 of 95.6%, and mAP@50–95 of 88.6%, thereby outperforming all other versions of YOLO that were analysed and showing strong competency.

Keywords: lunar crater detection; Chandrayaan-2; YOLO (You Only Look Once); SAM (Segment Anything Model); OHRC (Orbiter High Resolution Camera) imagery; lunar surface analysis; crater geometry estimation

1. Introduction

Lunar craters are among the most prominent features on the surface of the Moon and are considered to have great significance with respect to the chronological evolution of the surface of the Moon and other planets. It has become possible to study the structures of the craters on the surface of the Moon with greater detail and precision with the availability of high-resolution images of the Moon from the latest space missions, like Chandrayaan-2. It has become possible to observe the craters on the surface of the Moon with greater detail and precision with the availability of images from the Orbiter High Resolution Camera (OHRC), which offers submeter resolution with respect to the features on the surface of the Moon.

Despite the availability of good-quality information, the identification and measurement of lunar craters by hand prove to be a difficult task. Conventional methods for cataloguing lunar craters involve a high degree of manual annotation or semi-automated techniques. With the increasing amount of planetary image information, the conventional method of analysing planetary images by hand proves to be inefficient. Hence, the need for an automated system to identify the craters with good accuracy becomes a necessity.

Recent research in deep learning techniques has reported positive results in the detection of features within remote sensing images. Specifically, object detection techniques such as the YOLO algorithm have reported positive results in the detection of objects within complex visual environments. While the detection of potential crater locations can be done through object detection techniques, the results of these models are limited to bounding box predictions. For the accurate measurement of the properties of the crater, the results must be at the pixel level.

To overcome this limitation, segmentation-based methods can be integrated with detection-based methods to refine the boundaries of the detected craters. Recently, the computer vision domain has seen the development of the Segment Anything Model (SAM), which is a significant innovation for image segmentation with the least possible human interaction. Using this method, it is possible to achieve the detection of accurate boundaries for the craters.

In this work, we present an automated framework for the detection of craters on the Moon along with the geometric measurements of the craters based on high-resolution images acquired from the Chandrayaan2 OHRC payload. In the proposed framework, the YOLOv26 based detection framework is used to identify the craters' potential locations on the lunar surface. Then, the detected regions are further processed using the Segment Anything Model for obtaining the pixel-level segmentation of the craters. Further, the obtained segmentation results are then processed for estimating the geometric measurements of the craters.

2. Related work

Automated detection of lunar craters has been a research focus in planetary science and computer vision. This is because the statistics of the craters are important in understanding the geological evolution of the planetary bodies [1]. Initially, the techniques that were used to detect the craters on the moon were mainly those that used the conventional methods of image processing. For instance, edge detection techniques, circular Hough transform techniques, as well as template matching techniques, were the most commonly used techniques to detect the craters on the moon [1]. However, these techniques were limited in the sense that they could only be used to detect large and well-defined craters.

In recent years, with advancements in machine learning techniques, researchers started investigating data-driven techniques for crater detection. Convolutional Neural Networks (CNNs) were found to perform better in learning visual patterns related to the structure of craters [2]. Various researchers have employed deep learning techniques for automatic detection of craters using data related to planetary bodies, such as images from the Lunar Reconnaissance Orbiter and various lunar missions [2]. Such techniques were found to improve detection accuracy significantly compared to conventional image processing techniques. However, various CNN-based techniques were found to be limited to classification and patch detection, where accurate localization was not considered.

Recently, object detection models have been used for the automatic detection of craters. Among them, YOLO is found to have gained significant attention due to the accurate detection of objects in real-time [3]. YOLO-based methods have been used to effectively identify the positions of the crater in the image of the moon by predicting bounding boxes for the potential positions of the crater [3]. Real-time object detection system implementations for performing advanced visual analysis tasks have also been investigated by recent works. Modern advanced vision algorithms based on deep-learning techniques have shown higher efficiency and improved object detection results when applied to practical tasks, indicating the increased usefulness of object detection approaches in automated image analysis [4]. Though the YOLO-based methods have shown accurate crater detection methods, the bounding box does not represent the actual shape of the crater.

Modern research proves the efficiency of deep learning-based methods for object detection, which are used for solving complicated vision-based tasks, showing their ability to provide efficient feature extraction and accurate object localization. It additionally shows how powerful modern object detection models can be in terms of automating the process of image analysis [5,6].

To overcome this drawback, there is segmentation-based strategy for acquiring pixel-level information about crater boundaries. Various image segmentation techniques help to identify the region of the image corresponding to the craters at the pixel level. Recently, a novel foundation model known as the Segment Anything Model (SAM) has been proposed to generate high-quality segmentations for a broad range of vision domains [7]. Its ability to generate high-quality object boundary information makes it a promising technique for refining the region of the object detected by the object detection model.

Despite all these advancements, very few studies have employed the detection and segmentation approaches for the extraction of crater boundaries and the measurement of the geometrical features with high accuracy, especially through the use of high-resolution images provided by the Chandrayaan-2 Orbiter High Resolution Camera (OHRC) [8]. Unlike approaches that only consider detection or segmentation, the framework presented incorporates both object detection and segmentation approaches to achieve crater localization, boundary extraction, and geometrical measurements using a common framework.

Research into early craters mainly looked at topographic and shape-related data from planetary surfaces. Salamunicar and Lonacaric created a method using gradient analysis, digital topography, vote analysis, and calibration to find craters [9]. Recently, with the rise of foundation models, the Segment Anything Model (SAM) showed great promise in analyzing remote sensing images and planetary surfaces [10]. Subsequently, deep learning-based crater detection got a lot of focus. Zhu et al. suggested a YOLOv7 method boosted with CBAM for better lunar crater detection [11]. They then improved it by adding deformable convolutional networks to make feature extraction more robust [12]. Mane et al. did a comprehensive review of techniques for detecting lunar craters using image processing and pointed out some research challenges [13].

Jia et al., on the other hand, looked into automated crater detection with deep learning for analyzing the Moon's surface [14]. Additionally, Sinha and Paul gave a detailed review that included insights from Chandrayaan-2's TMC-2 observations [15].

High-quality lunar datasets have really advanced automated crater detection systems. The Chandrayaan-2 OHRC payload, for instance, offers superb high-res lunar images great for detailed crater studies [16]. We also get helpful data from the Lunar Reconnaissance Orbiter and its camera [17, 18]. Besides that, there are public datasets such as the Lunar Crater Detection Dataset, the PRADAN planetary archive, the Moon Crater Database version one, and NASA's OHRC records [19–22]. These resources seriously support the research community in this field. Recent progress includes SAM 3 and flexible frameworks that use SAM for accurate crater boundary extraction [23, 24]. Also, some reviews highlight the recent advances in using deep learning to spot craters on the moon [25]. Plus, high-res OHRC images aid geological research, such as studying boulder groups near fresh craters [26]. These studies show how crater detection evolved from old image-processing methods to today's advanced deep learning and foundation models. Additionally, some folks are still using those older techniques, but progress has been pretty huge.

3. Dataset

The dataset used for the research for this paper consists of high-resolution images of the moon taken by the Orbiter High Resolution Camera (OHRC) carried by Chandrayaan-2. OHRC allows for extremely high spatial resolution images to be taken of the lunar surface. These images can be used to observe small-scale geological features of the moon's surface, including impact craters. The spatial resolution of the images taken by OHRC amounts to 0.25 m per pixel from an altitude of 100 km. It provides a 3 km swath with a panchromatic band making it the highest camera on any lunar mission.

The study area considered includes specific areas on the Moon's surface, where the formation of craters is visible and identifiable through the images provided by the OHRC. These images have various forms and sizes of craters, making it possible to assess the effectiveness of the automated crater detection and segmentation approaches. The high resolution of the images enables the identification of small craters on the moon's surface.

Due to the large size of the images from the OHRC dataset, preprocessing is necessary before the detection model can be applied. Images from the dataset have very large spatial dimensions, making the processing computationally expensive. A total of around 12,000 image patches were produced from the OHRC lunar images dataset after preprocessing. Every image patch has a dimension of 640×640 pixels for training the model. The obtained data set was partitioned into training, validation, and testing sets in the ratio of 70:20:10 respectively.

The object detection model used in this research is trained with the high-resolution lunar images obtained from the Orbiter High Resolution Camera, which is a part of the Chandrayaan-2 mission. The OHRC dataset is retrieved from the PRADAN Portal, which is used to distribute the planetary mission data from the Indian Space Research

Organization. The dataset is a collection of high-resolution images of the lunar surface with varying structures of craters. These images are then annotated with bounding box labels that identify the location of the craters. Each bounding box label is defined as a normalized bounding box with the class identifier of the crater along with the coordinates.

Once the training phase was completed, the trained model was used to classify the other set of high-resolution lunar images captured by the Orbiter High Resolution Camera (OHRC) on the Chandrayaan-2 satellite. The trained model detected the potential locations of the craters from the OHRC images, which were stored for future analysis.

4. Methodology

This study proposes an automated framework that can be used to carry out crater detection and geometric analysis on the lunar surface using high-resolution lunar imagery of Chandrayaan-2. As shown in **Figure 1**, the proposed methodology uses object detection and segmentation techniques to accurately identify the locations of the craters as well as their boundaries. The workflow of the proposed framework can be divided into four major stages.

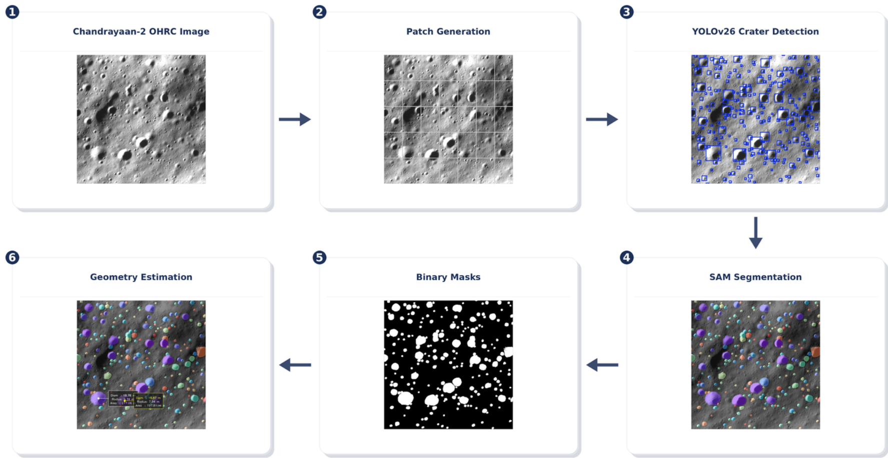

Figure 1. Proposed Framework.

4.1. Patch generation

The images obtained by the Orbiter High Resolution Camera (OHRC) onboard the Chandrayaan-2 spacecraft are of very large spatial dimensions. It is not efficient to process images of large dimensions using deep learning models. As shown in **Figure 2**, to solve this problem, the images obtained by the OHRC are split into patches before they are processed by the deep learning models. Splitting the images into patches is an efficient way to process large images without compromising the important visual details required to detect craters in the images. Each patch is processed separately by the model to generate the final crater detection results.

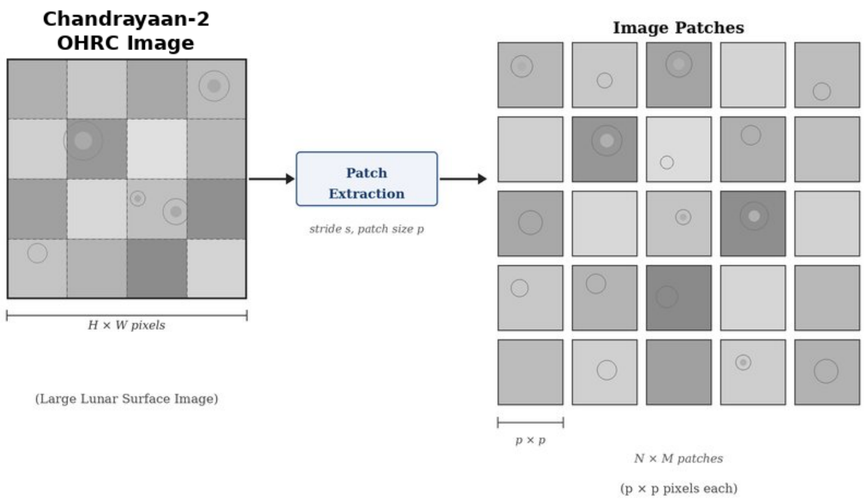

Figure 2. Patch Generation.

4.2. Crater detection using YOLOv26

Crater detection is made possible through the use of the YOLO framework. This framework is widely utilized as an object detector because of its ability to simultaneously localize objects while classifying them.

Figure 3 is an architecture representation of the YOLOv26 model used in this research. The YOLOv26 model makes use of the backbone for feature extraction at different levels, neck for multi-scale information aggregation, and detection head for object localization and classification.

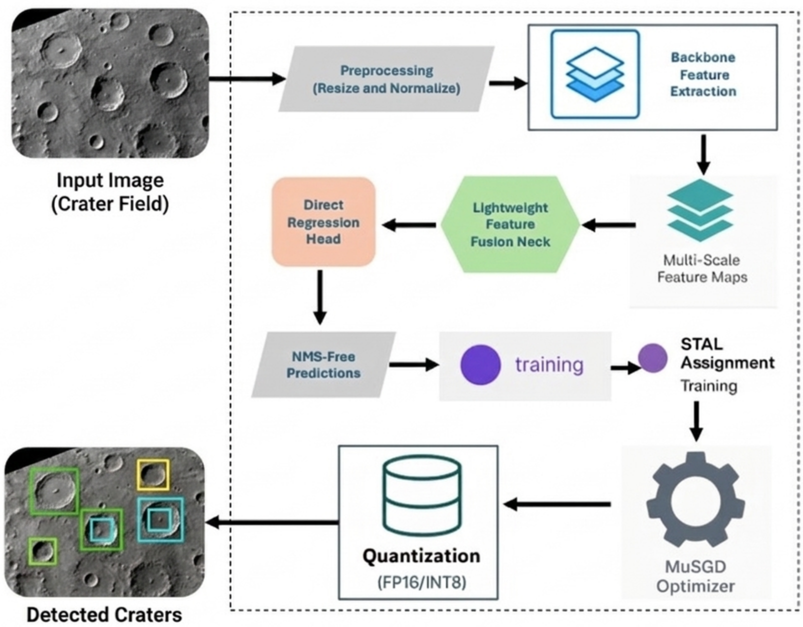

Figure 3. YOLOv26 Architecture.

The model that was developed for the study uses images captured by the Orbiter High Resolution Camera (OHRC) of the Chandrayaan-2. The image samples were downloaded from the PRADAN data portal and contain visual information of the moon at high resolution. Crater-specific visual features were then learned by the model in conjunction with predicting crater localization using bounding boxes.

The OHRC images were preprocessed into smaller images known as image patches. These image patches are necessary to make the processing and evaluation faster. Each image patch is then analyzed individually using the YOLOv26 model.

Through this method, the YOLOv26 model provides predictions of the location of the craters by outputting bounding boxes on the potential areas where craters are found.

The model was trained for 200 epochs with a batch size of 8 in a CUDA-enabled GPU environment. Python version 3.13 was used alongside various deep learning libraries such as PyTorch and Ultralytics libraries. Performance measures include Precision, Recall, mAP@50, and mAP@50–95.

Even though the generated bounding boxes can reliably localize the craters, they define the craters by using rectangular boxes. Hence, a segmentation phase is needed to derive the exact crater boundaries.

Selection of YOLOv26 and model architecture

The YOLOv26 model was chosen for the detection of craters because of its advanced end-to-end detection, efficiency, and performance in detecting small objects. The detection of craters from lunar images is a challenge because of the varying sizes and edge features, as well as illumination. However, YOLOv26 was chosen because of its higher accuracy in small object detection, lower computational cost, and better feature aggregation. This model was more appropriate to detect small moon craters in high-resolution images captured from the OHRC camera.

Unlike other object detection approaches, the YOLOv26 architecture is based on a non-maximum suppression (NMS) free object detection paradigm, which allows for end-to-end learning to take place. Instead of producing multiple predictions and then eliminating redundant detections, the model is designed to produce a single high-confidence object detection per object. This is made possible through a one-to-one label assignment, which internally eliminates redundant detections during training, thus being beneficial when dealing with large OHRC image patches.

The architecture of YOLOv26 comprises three major parts: the backbone, the neck, and the detection head. The backbone of the YOLOv26 network is in charge of learning the hierarchical representations of the input image, which includes not only the low-level features like edge and gradient information but also the high-level semantic features like the circular rims of the craters, the shadow illumination patterns, and the texture changes on the surface.

The neck component is used for multi-scale feature aggregation through feature pyramid representations. This is useful for detecting craters of different scales. This is especially useful for images from OHRC, where craters can be of different scales within one image. The multi-scale feature fusion helps to maintain spatial details and contextual information.

The detection head directly predicts bounding box parameters from feature maps. Each prediction contains parameters such as center coordinates (x, y), width (w), height (h), and object confidence. YOLOv26 eliminates the need for DFL in bounding box regression and provides a stable and direct prediction of object locations.

Furthermore, YOLOv26 has employed sophisticated training techniques such as Progressive Loss Balancing and Small Target Aware Label Assignment (STAL), which improve detection accuracy. The model was developed based on OHRC crater image patches and their performance were evaluated based on Precision, Recall, mAP@50, and mAP@50–95 evaluation criteria.

Overall, the choice of YOLOv26 is beneficial for efficient and accurate crater detection, allowing for the reliable localization of crater regions without compromising a highly efficient and end-to-end crater detection pipeline.

4.3. Crater segmentation using SAM

For accurate delineation of the craters' boundaries, the identified crater areas are then refined by performing segmentation with the help of the Segment Anything Model. The Segment Anything Model (SAM) is an artificial intelligence system used to perform precise image segmentation regardless of visual domain.

Figure 4 illustrates the architecture of the SAM3 model employed in this work. The model extracts high-level visual representations through the image encoder, incorporates user or detection prompts using the prompt encoder, and generates accurate pixel-level segmentation masks through the mask decoder.

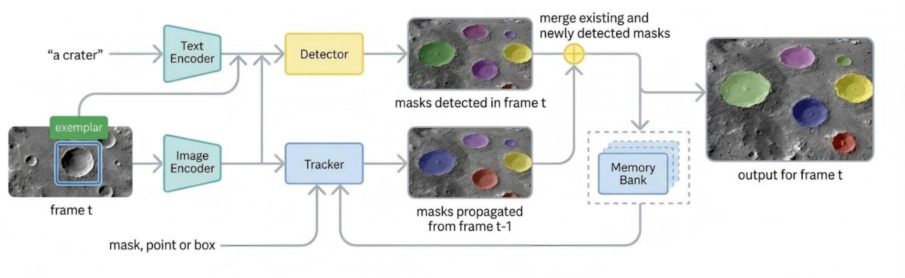

Figure 4. SAM3 Architecture.

The reason behind choosing SAM as a tool in this research lies in the strong generalization ability, prompt-based image segmentation process, and generating precise pixel-level object segmentation boundaries without any need for retargeting the image segmentation model with task-specific training in different image situations. The images taken from the lunar surface exhibit substantial differences related to lighting conditions, texture of the surface, distribution of shadows, and morphological properties of craters. The standard image segmentation techniques usually rely on vast quantities of manually labelled pixel-level training data and may fail at generalizing due to the lack of similar terrain conditions.

The second important advantage of the SAM model is that it allows for fine-tuning coarse object detection results to accurate object boundaries. In fact, the crater regions identified with the help of the YOLOv26 model give only the rectangular localization of objects by means of bounding boxes and do not provide accurate representation of the true object geometry. Since crater measurements require morphological information, pixel segmentation is important. With this respect, SAM overcomes the limitations of YOLOv26 by providing accurate segmentation masks along the rim of the crater and inside it.

To solve this problem, the regions inside the detected bounding boxes are used as inputs for the segmentation model. The SAM segmentation model uses the prompt-based architecture for generating pixel segmentation masks that correspond to crater boundaries. The model comprises three modules, including an image encoder, prompt encoder, and mask decoder. Image encoding helps in extracting visual features from images, while prompt encoding takes into account spatial hints of bounding boxes and generates segmentation masks.

Segmentation plays a vital role in improving the accuracy of the detected output because it replaces inaccurate rectangles of craters with precisely segmented crater forms. This is very useful when it comes to partially damaged and distorted crater structures in the images taken from the Moon's surface where an exact outline can't be found via bounding box detection.

Such segmentation will help to improve geometric properties of craters, like crater radius and diameter.

4.4. Crater geometry estimation

Once the segmentation masks for the detected craters are obtained, the geometric properties of the detected craters are estimated by making pixel-based measurements. Using the segmentation masks for the detected craters, the exact region of the image corresponding to the detected crater can be identified.

The diameter of the detected crater can be estimated by measuring the maximum distance across the region of the image defined by the segmentation mask for the detected crater. Similarly, the radius of the detected crater can be estimated by calculating half the estimated diameter of the detected crater. Moreover, the surface area of the detected crater can be estimated by making a count of the pixels contained within the region defined by the segmentation mask for the detected crater.

To convert the estimated measurements for the detected crater from pixels to actual physical units, the scale of the pixels in the OHRC images (0.25 m/pixel) can be used.

4.4.1. Pixel level measurements

At the pixel level, the measurements are directly calculated based on the segmentation masks. The diameter of a crater is calculated as the maximum distance over its segmented boundary, whereas the radius is half of that. The area of a crater is given by the number of pixels in its segmented region.

Diameter (pixel level): The diameter of the crater is defined as the maximum distance present between two points on the segmented boundary of the crater. It is calculated as:

$$D_{\text{pixel}} = \max(d_x, d_y), \tag{1}$$

where d_{x} and d_{y} are the horizontal and vertical distances across the boundary, respectively.

Radius (pixel level): The radius is simply half of the diameter:

$$R_{\text{pixel}} = \frac{D_{\text{pixel}}}{2}. \tag{2}$$

Area (pixel level): The surface area of the crater is determined by counting the number of pixels contained within the segmentation mask. The area is given by:

$$A_{\text{pixels}} = N_{\text{pixels}}, \tag{3}$$

where N_{pixels} is the total number of pixels within the segmented region.

4.4.2. Real world measurements

To transform the pixel-based measurement into real-world units, the pixel scale of the OHRC image is used. In the case of the Chandrayaan-2 OHRC image, the pixel scale is 0.25 meters per pixel. By using the pixel scale, the measurements of the image can be converted.

Diameter (real world): The diameter Dreal can be calculated by multiplying the pixel level diameter by the pixel scale:

$$D_{\text{real}} = D_{\text{pixel}} \times \text{Pixel Scale}, \tag{4}$$

where the pixel scale is 0.25 m/pixel.

Radius (real world): The real-world radius Rreal is calculated as:

$$R_{\text{real}} = R_{\text{pixel}} \times \text{Pixel Scale}. \tag{5}$$

Area (real world): The real-world surface area Areal is calculated by converting the pixel area to square meters:

$$A_{\text{real}} = A_{\text{pixel}} \times (\text{Pixel Scale})^2. \tag{6}$$

The equation converts the area from pixels to square meters using the square of the pixel scale.

However, the geometrical parameterization method relies on the assumptions that the extracted craters' outline is accurate and that the OHRC image scale is constant for the whole image area under study. The changes in lighting, the nature of the crater, or an inaccurate extraction might affect the estimation accuracy.

5. Experimental results

This section reports the experimental results obtained using the proposed lunar crater detection and measurement approach. In this work, experiments have been carried out on high-resolution lunar images obtained by the Orbiter High Resolution Camera (OHRC) carried by Chandrayaan-2. In the experiments, the potential of the proposed approach in accurately detecting the location of the crater and determining their geometrical characteristics is tested.

5.1. Crater detection results

The detection of craters was achieved by utilizing the YOLO object detection algorithm. The object detection model was used to detect craters on the OHRC image patches that were generated during the image preprocessing phase.

The detection results indicate that the object detection model has successfully identified multiple crater structures in various regions of the lunar surface. The predicted bounding boxes represent the initial location of the craters on the lunar surface, which are used as input for the segmentation phase.

Figure 5 shows the crater detection results achieved by utilizing the YOLO object detection model, where the bounding boxes represent the location of the craters on the OHRC image patches.

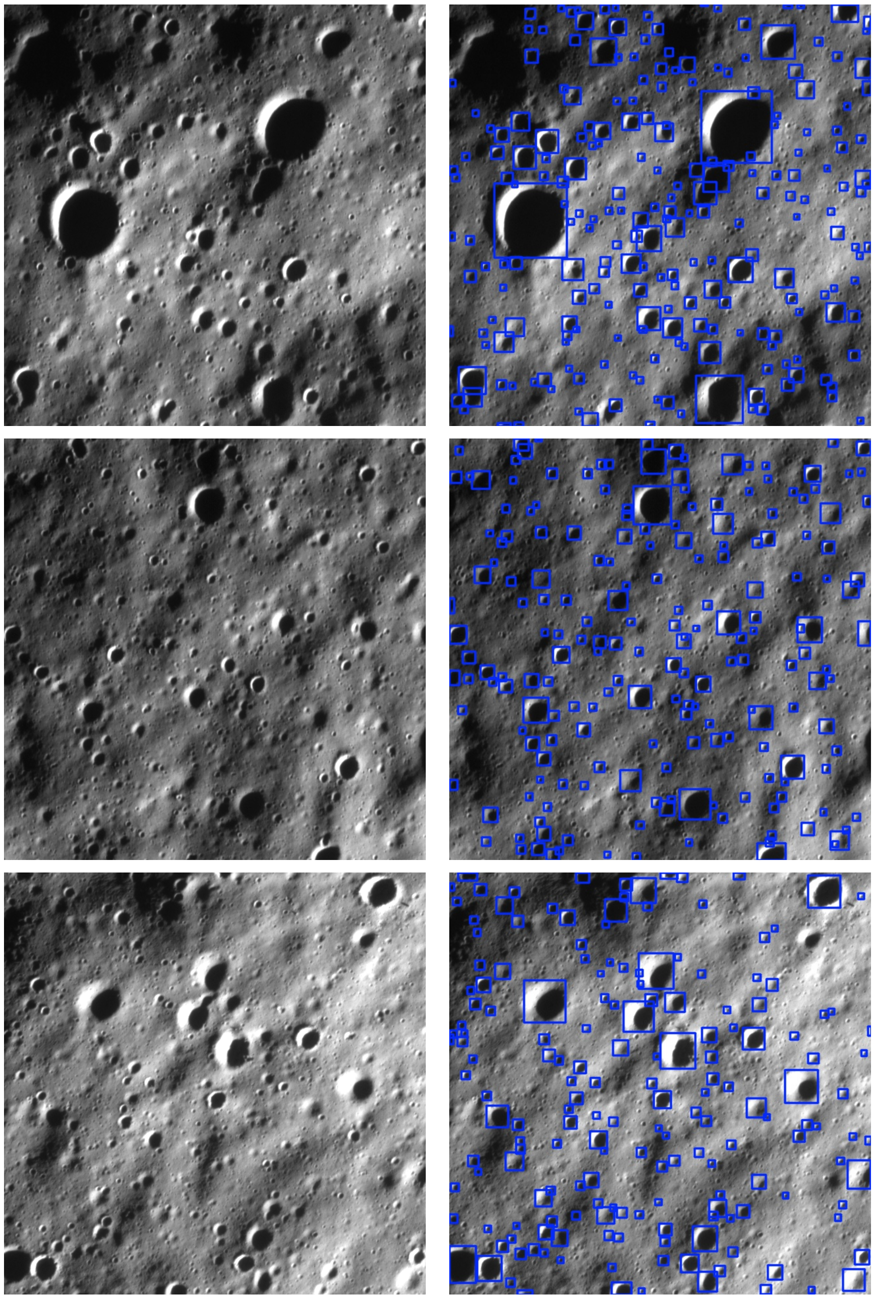

(a) Examples 1–3.

Figure 5. *Cont.*

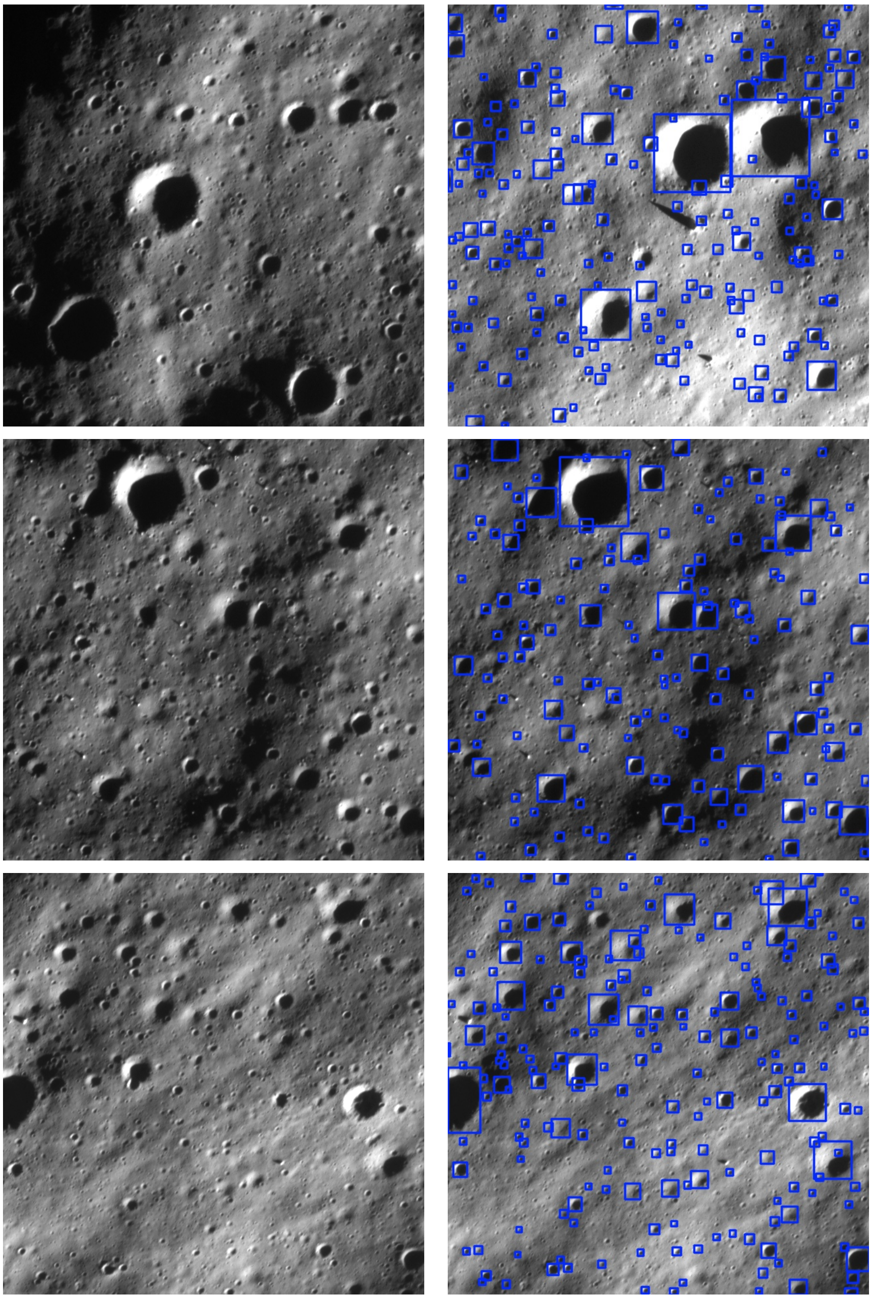

(b) Examples 4–6.

Figure 5. YOLOv26 Crater Detection Results.

5.2. Crater segmentation results

To get accurate boundaries of the detected crater regions, further processing of the detected regions was carried out by using the Segment Anything Model. For each detected region, the input to the segmentation model was provided by specifying the image region corresponding to each detected bounding box. The segmentation model uses masks that represent the boundaries of the crater regions. This representation of the crater regions is more accurate compared to the use of bounding boxes. **Figure 6** shows the representation of the segmentation masks obtained from the segmentation model, which indicates the boundaries of the detected crater regions.

5.3. Crater geometry measurement

Following the segmentation stage, the geometric properties of the detected craters were determined using pixel-based geometric calculations. The segmentation mask for each crater indicates the exact region covered by each pixel, thus enabling accurate computation of the size and area of each crater. The diameter of each crater is determined by computing the maximum distance covered by each pixel within the crater segmentation mask, while the radius is determined as half the diameter. The surface area of each crater is determined as the total number of pixels contained within the segmentation mask for each crater. In order to obtain the crater geometric properties in real-world units, the pixel resolution for the OHRC image, which is about 0.25 m, was used. The crater geometric properties include diameter, radius, and surface area. **Figure 7** shows the crater geometry measurement results.

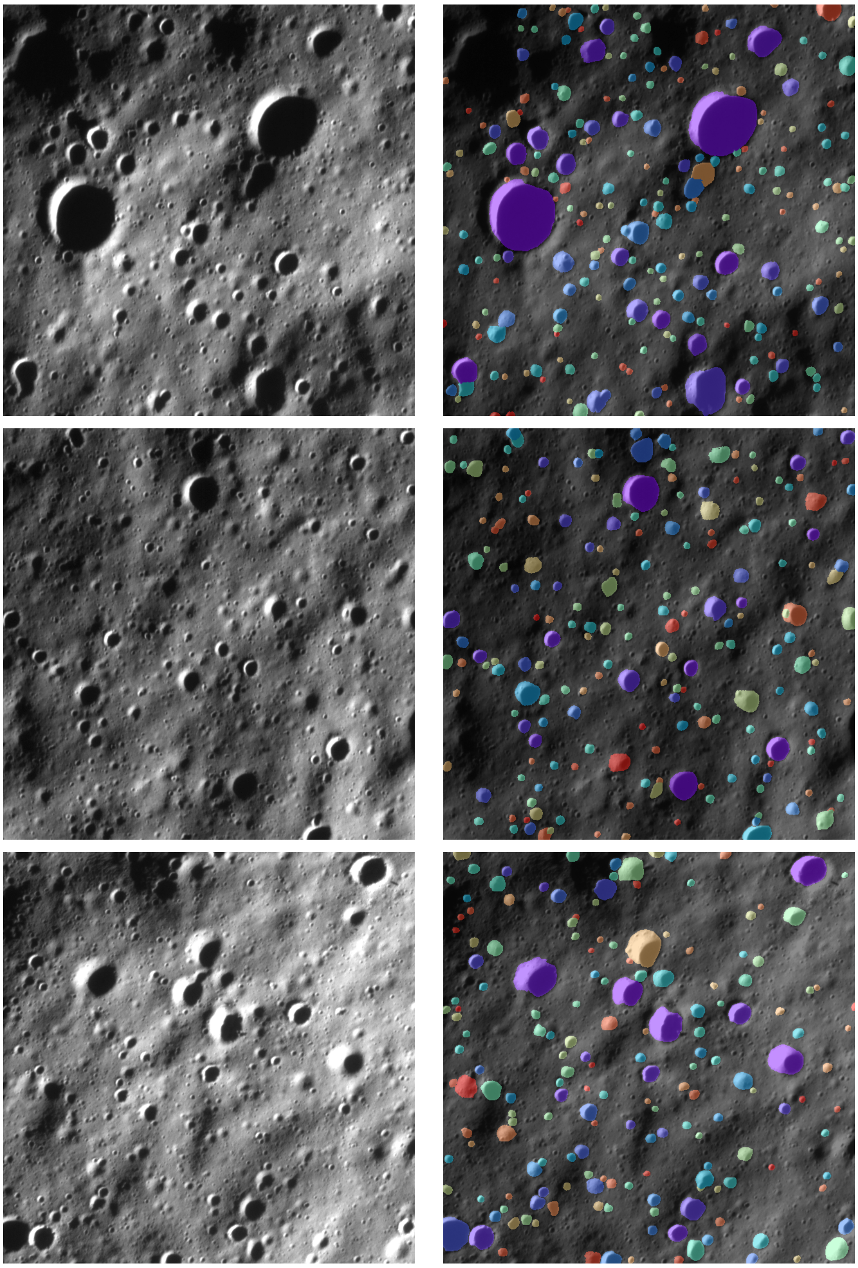

(a) Examples 1–3.

Figure 6. *Cont.*

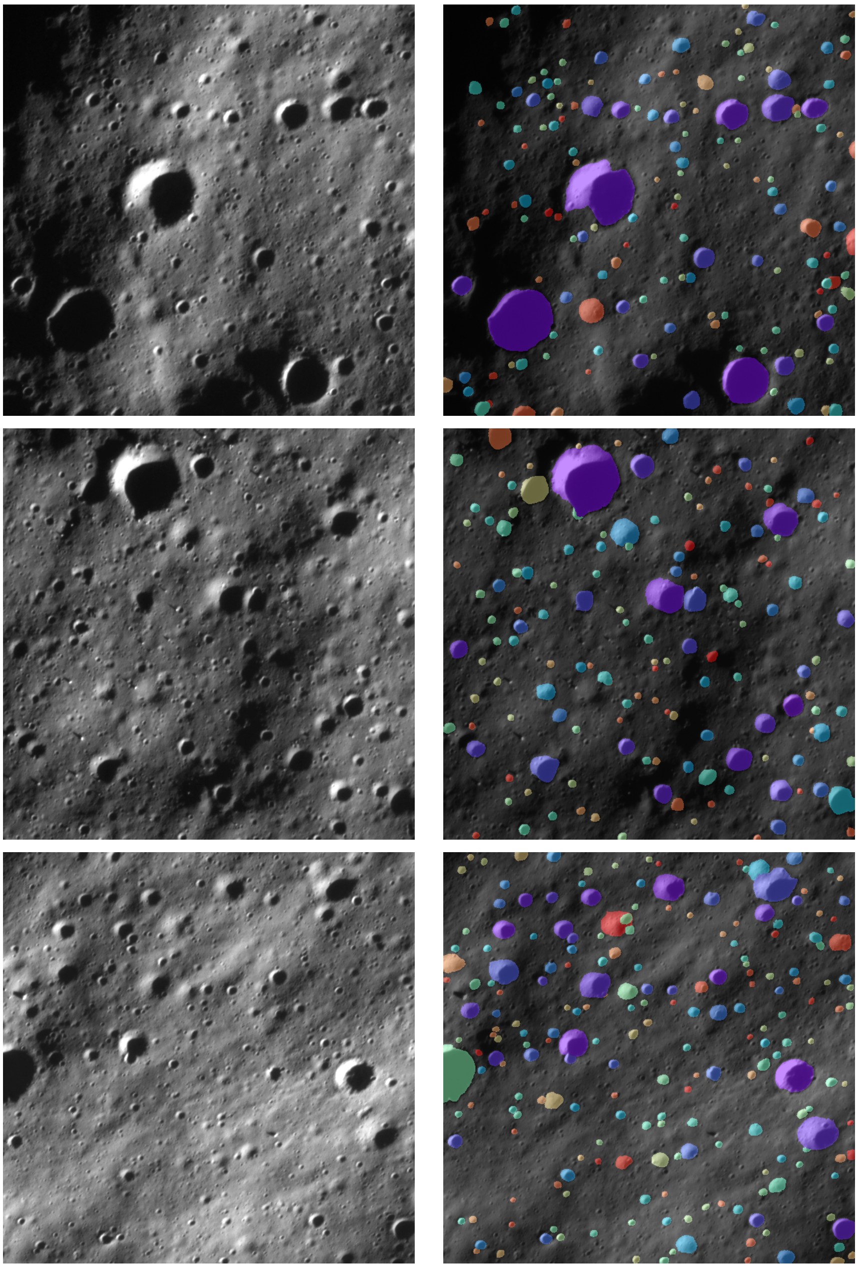

(b) Examples 4–6.

Figure 6. Crater Segmentation Results.

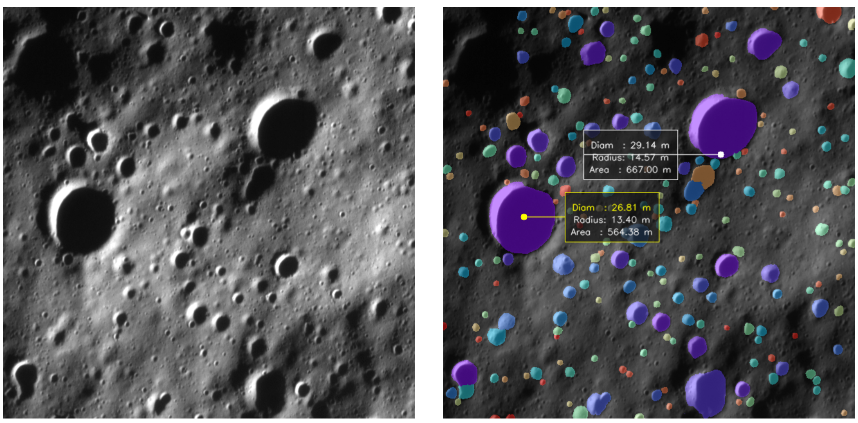

Figure 7. *Cont.*

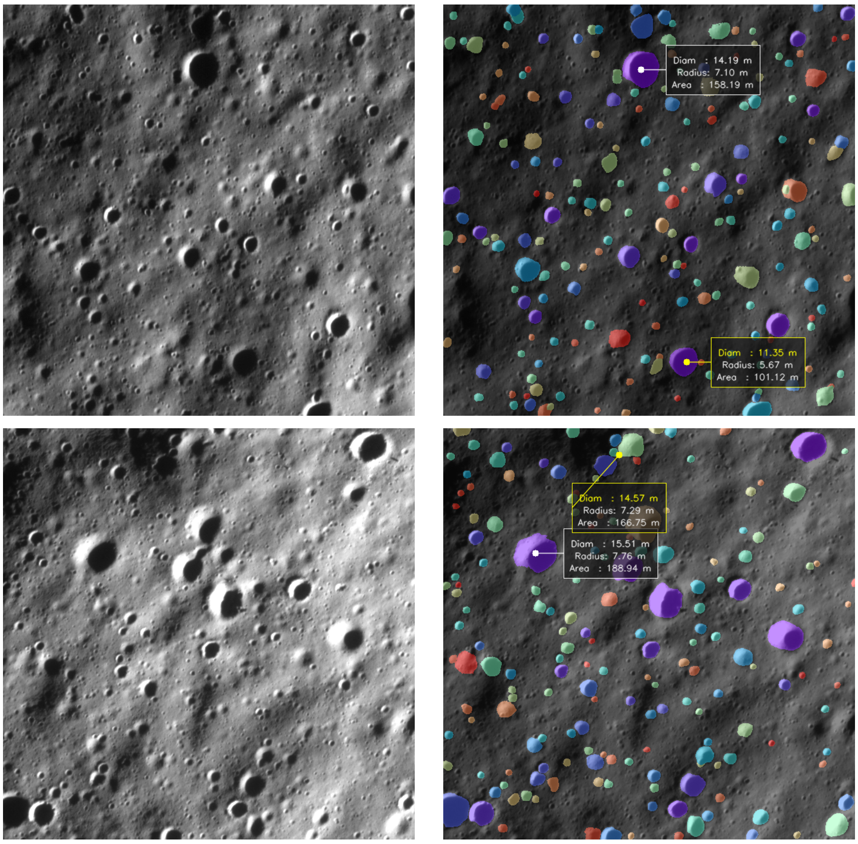

(a) Examples 1–3.

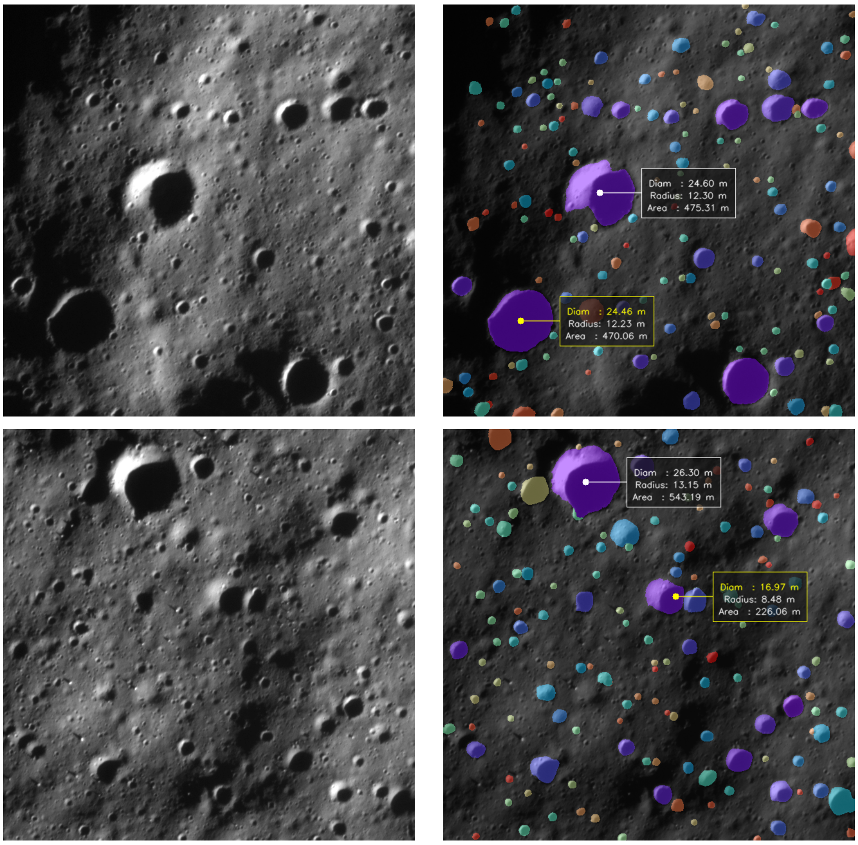

Figure 7. *Cont.*

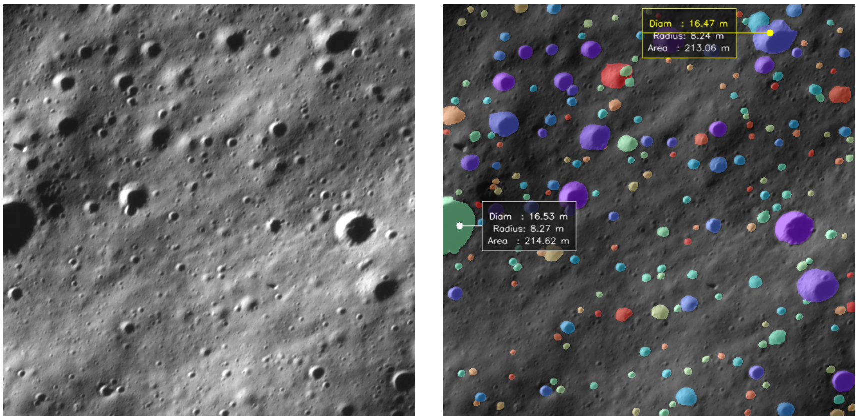

(b) Examples 4–6.

Figure 7. Crater Geometry Measurement Results.

6. Evaluation metrics

To evaluate the performance of the proposed framework for crater detection and segmentation, some standard performance metrics were used. The performance metrics were used to evaluate the accuracy and reliability of the obtained results for crater detection and segmentation using high-resolution lunar image data captured by the Orbiter High Resolution Camera (OHRC) installed on the Chandrayaan-2.

6.1. Detection metrics

For the purpose of evaluating the performance of the YOLO model on the crater detection task, various metrics that are commonly used in object detection tasks, such as Precision, Recall, F1-score, mean Average Precision (mAP), and mean Average Precision at an IoU threshold of 0.5 (mAP@0.5), were considered. Precision measures the proportion of correctly detected craters among all predicted detections. It is defined as:

$$\text{Precision} = \frac{TP}{TP + FP}, \tag{7}$$

where TP represents True Positives, FP represents False Positives Recall measures the proportion of actual craters that are correctly detected by the model. It is defined as:

$$\text{Recall} = \frac{TP}{TP + FN}, \tag{8}$$

where FN represents False Negatives.

F1-Score provides a balanced measure of detection performance by combining precision and recall. It is defined as:

$$\text{F1-Score} = 2 \times \frac{\text{Precision} \times \text{Recall}}{\text{Precision} + \text{Recall}}. \tag{9}$$

In addition to the above parameters, mean Average Precision (mAP) is used to assess the entire detection performance of the model at different Intersection over Union (IoU) levels. mAP represents the entire precision-recall curve. mAP@0.5 (mAP50) refers to the mean Average Precision at an IoU threshold of 0.5, where a detection is considered to have been made if the predicted bounding box overlaps at least 50%

with the ground truth. A higher mAP and mAP50 indicate a higher crater detection performance.

6.2. Segmentation metrics

The segmentation stage is carried out to improve the accuracy of the crater detection and to obtain the boundaries of the craters from the detected regions. For this purpose, the detected regions in the form of bounding boxes, which are provided by the YOLO detector, are used to create the input prompts to the model called the Segment Anything Model (SAM).

From the qualitative results, it is evident that the segmentation model successfully identifies the circular and irregular shapes of the lunar crater features as seen in the OHRC images obtained through the Chandrayaan-2 satellite. The precision of the crater features is more accurate using the segmentation mask as compared to the bounding box.

In **Figure 6**, the segmentation output is shown as an example, in which the generated masks have successfully distinguished the crater rims and inner regions. The crater boundaries extracted in this method allow for further analysis of the crater's shape compared to the bounding box method.

Geometric properties of the craters are estimated based on the segmentation masks. The diameter of the craters is estimated by finding the maximum distance across the segmented region of the craters. The radius of the craters is estimated as half the diameter. The surface area of the craters is estimated by counting the number of pixels within the segmentation mask and converting the result into real-world units based on the pixel scale of the OHRC.

These measurements enable the extraction of significant characteristics of the craters such as diameter, radius, and surface area. These are significant parameters for the study of the planetary surfaces.

6.3. Comparative study

This section provides a comparative evaluation of the proposed crater detection framework based on YOLOv26 with other techniques that have been presented in the literature. For this purpose, the proposed technique is compared with other techniques based on Precision, Recall, and F1-Score, and Mean Average Precision (mAP).

In order to establish a level playing field for comparison of performance among different YOLO versions, all the YOLO variants used for performance comparison were trained and tested under identical experimental settings (**Table 1**).

Table 1. Comparative Study.

Models	Precision (%)	Recall (%)	mAP@0.5 (%)	mAP@0.5:0.95 (%)
YOLOv5	86.3	79.5	86.7	77.7
YOLOv8	90.2	74.4	87.4	78
YOLOv11	81.9	81.6	88.5	78.4
YOLOv12	83.2	84.9	88.9	79.3
YOLOv26 (proposed method)	**91.5**	**88.6**	**95.6**	**88.6**

The results obtained indicate that the proposed approach yields better results compared to existing methods of detecting craters. The incorporation of YOLOv26 is effective in detecting the location of craters, while the next segment of the process is effective in providing accurate geometric analysis.

In addition, the NMS-free detection method in YOLOv26 improves the accuracy of prediction and consistency in detection. Furthermore, the addition of the segmentation-based refinement helps to achieve more accurate delineation of the boundary of the craters. This cannot be done using the bounding box-based approach.

On the whole, the suggested approach shows good results in terms of accuracy and geometrical measurements, making it applicable to the analysis of large-scale lunar surfaces based on high-resolution images taken by Chandrayaan-2.

7. Conclusion

This paper proposed a framework for automated detection and geometric measurement of lunar craters based on highresolution images obtained by the Orbiter High Resolution Camera (OHRC) installed in Chandrayaan-2. In this proposed framework, YOLO is used for crater detection and the Segment Anything Model for accurate crater boundary detection. With the use of segmentation masks, it is possible to estimate crater geometric properties such as diameter, radius, and surface area based on pixel measurements and scale conversion.

This YOLOv26 model gave a precision value of 91.5%, a recall of 88.6%, mAP@50 of 95.6%, and mAP@50–95 of 88.6%. The results of the experiments prove the effectiveness of the proposed framework in the detection of crater structures and the extraction of the boundary details of the detected craters from the high-resolution images of the Moon. The proposed framework is a viable solution for the automated analysis of the surfaces of planets and the Moon. The proposed method is an advancement over the existing bounding box-based approaches. Although the suggested algorithm has shown its efficiency, some limitations still exist in the SAM-based segmentation step. For example, the segmentation step might be impacted by areas including low-contrast craters' boundaries, overlapping craters, or highly varying shadows within OHRC images. Moreover, the quality of the output segmentations depends on the quality of the initial detections made using YOLOv26, because inaccuracies in detecting objects' boundaries might affect further steps.

In addition, the current study mainly analyses the performance of the crater detection stage by applying conventional object detection metrics. In future research, efforts will be made to create annotated datasets for the segmentation stage analysis.

Future research could address issues related to increasing the robustness of detection under different illumination conditions, as well as using other data sources such as Digital Elevation Model (DEM) data, which could help improve crater characterization, such as crater depth estimation and 3D crater morphology. Future research could also address issues related to creating a generalized crater analysis model, which could help identify various types of craters, such as simple, complex, and degraded craters, depending on their morphology. This could help expand lunar surface research, providing further insights into impact phenomena and geological evolution of celestial bodies.

Author contributions: Conceptualization, MS and PG; methodology, MS; software, PG; validation, PG and MS; formal analysis, PG; investigation, PG; resources, MS; data curation, PG; writing—original draft preparation, PG and MS; writing—review and editing, MS and PG; visualization, PG; supervision, MS; project administration, MS. Both authors have read and agreed to the published version of the manuscript.

Funding: This research and manuscript were conducted without any external funding.

Institutional review board statement: Not applicable. This study has been carried out on Open Free datasets and does not involve human participants, animals or any form of personal data.

Informed consent statement: Not applicable. This study has been carried out on Open Free datasets and does not involve human participants, animals or any form of personal data.

Data availability statement: The data used for this research were gathered from the PRADAN website of the Indian Space Research Organization (ISRO). The original datasets can be accessed via the PRADAN website according to the policies of PRADAN regarding accessing its data.

Conflict of interest: The authors declare no conflict of interest.

AI use statement: During the preparation of this work, the authors used AI tools to assist with language refinement, grammar improvement, manuscript organization, and editing. All the suggestions provided by the tools were reviewed and the authors take full responsibility for the final content of the published article.

References

1. Silburt A, Ali-Dib M, Zhu C, et al. Lunar crater identification via deep learning. Icarus. 2019; 317: 27–38. doi: 10.1016/j.icarus.2018.06.022
2. Lee C. Automated crater detection on Mars using deep learning. Planetary and Space Science. 2019; 170: 16–28. doi: 10.1016/j.pss.2019.03.008
3. Bochkovskiy A, Wang CY, Liao HYM. YOLOv4: Optimal Speed and Accuracy of Object Detection. arXiv preprint. 2020. doi: 10.48550/ARXIV.2004.10934
4. Zhang S, Zhang P, Yang J, et al. Automatic detection for small-scale lunar impact crater using deep learning. Advances in Space Research. 2024; 73(4): 2175–2187. doi: 10.1016/j.asr.2023.05.041
5. Güney E, Bayılmış C, Çakar S, et al. Autonomous control of shore robotic charging systems based on computer vision. Expert Systems with Applications. 2024; 238: 122116. doi: 10.1016/j.eswa.2023.122116
6. Guney E, Bayilmis C, Cakan B. An Implementation of Real-Time Traffic Signs and Road Objects Detection Based on Mobile GPU Platforms. IEEE Access. 2022; 10: 86191–86203. doi: 10.1109/ACCESS.2022.3198954
7. Kirillov A, Mintun E, Ravi N, et al. Segment Anything, in: 2023 IEEE/CVF International Conference on Computer Vision (ICCV). In: Proceedings of the 2023 IEEE/CVF International Conference on Computer Vision (ICCV); 1–6 October 2023; Paris, France. pp. 3992–4003. doi: 10.1109/ICCV51070.2023.00371
8. Indian Space Research Organisation (ISRO). Chandrayaan2. ISRO; 2019. Available online: https://www.isro.gov.in/Chandrayan_2.html
9. Salamuniccar G, Loncaric S. Method for Crater Detection From Martian Digital Topography Data Using Gradient Value/Orientation, Morphometry, Vote Analysis, Slip Tuning, and Calibration. IEEE Transactions on Geoscience and

Remote Sensing. 2010; 48(5): 2317–2329. doi: 10.1109/TGRS.2009.2037750
10. Osco LP, Wu Q, De Lemos EL, et al. The Segment Anything Model (SAM) for remote sensing applications: From zero to one shot. International Journal of Applied Earth Observation and Geoinformation. 2023; 124: 103540. doi: 10.1016/j.jag.2023.103540
11. Zhu J, Liang J, Tian X, et al. A Deep Learning Approach for Lunar Impact Crater Detection Based on YOLO v7 and CBAM Attention Mechanism. In: Proceedings of the 2023 8th International Conference on Intelligent Computing and Signal Processing (ICSP); 21–23 April 2023; Xi'an, China. pp. 2078–2081. doi: 10.1109/ICSP58490.2023.10248664
12. Chen S, Liang J, Zhu J, et al. New Methods for Lunar Impact Crater Detection Based on YOLO v7 with Deformable ConvNets. In: Proceedings of the 2023 IEEE International Conference on Electrical, Automation and Computer Engineering (ICEACE); 29–31 December 2023; Changchun, China. pp. 123–127. doi: 10.1109/ICEACE60673.2023.10442883
13. Mane O, Nagawade P, Pathak M, et al. A Comprehensive Review on Lunar Crater Detection using Image Processing. In: Proceedings of the 2025 Emerging Technologies for Intelligent Systems (ETIS); 7–9 February 2025; Trivandrum, India. pp. 1–5. doi: 10.1109/ETIS64005.2025.10961063
14. Jia Y, Wan G, Liu L, et al. Automated Detection of Lunar Craters Using Deep Learning. In: Proceedings of the 2020 IEEE 9th Joint International Information Technology and Artificial Intelligence Conference (ITAIC); 11–13 December 2020; Chongqing, China. pp. 1419–1423. doi: 10.1109/ITAIC49862.2020.9339179
15. Sinha M, Paul S. Automated detection of craters on the lunar surface using deep learning: A review with insights from Chandrayaan-2 TMC-2 data. Results in Earth Sciences. 2025; 3: 100094. doi: 10.1016/j.rines.2025.100094
16. Indian Space Research Organisation (ISRO). Chandrayaan2 Complete Project Payloads. Available online: https://www.isro.gov.in/chandrayaan2-payloads.html (accessed on 19 January 2026).
17. National Aeronautics and Space Administration (NASA). Lunar Reconnaissance Orbiter. NASA; 2009. Available online: https://www.nasa.gov/mission_pages/LRO/main/index.html
18. Lunar Reconnaissance Orbiter Camera (LROC). Available online: https://www.lroc.asu.edu/ (accessed on 21 January 2026).
19. La Grassa R. Impact Moon Craters (LU3M6TGT). Kaggle; 2023. Available online: https://www.kaggle.com/datasets/riccardolagrassa/lu3m6tgt
20. PRADAN. ISRO Science Data Archive (ISDA). Available online: https://pradan.issdc.gov.in (accessed on 19 January 2026).
21. Robbins S. Moon Crater Database v1 Robbins. USGS Astrogeology Science Center; 2018. Available online: https://astrogeology.usgs.gov/search/map/moon_crater_database_v1_robbins
22. NASA Space Science Data Coordinated Archive (NSSDCA), NASA. Chandrayaan-2 OHRC Instrument. NSSDCA, NASA; 2019.
23. Carion N, Gustafson L, Hu YT, et al. SAM 3: Segment Anything with Concepts. arXiv preprint. 2025. doi: 10.48550/ARXIV.2511.16719
24. Giannakis I, Bhardwaj A, Sam L, et al. A flexible deep learning crater detection scheme using Segment Anything Model (SAM). Icarus. 2024; 408: 115797. doi: 10.1016/j.icarus.2023.115797
25. Chaini C, Jha VK. A review on deep learning-based automated lunar crater detection. Earth Science Informatics. 2024; 17(5): 3863–3898. doi: 10.1007/s12145-024-01396-2
26. Dagar AK, Rajasekhar RP, Nagori R. Analysis of boulders population around a young crater using very high resolution image of Orbiter High Resolution Camera (OHRC) on board Chandrayaan-2 mission. Icarus. 2022; 386: 115168. doi: 10.1016/j.icarus.2022.115168